

A Gaussian Copula Approach to the Performance Analysis of Fluid Antenna Systems

Farshad Rostami Ghadi, Kai-Kit Wong, *Fellow, IEEE*, F. Javier López-Martínez, *Senior Member, IEEE*, Chan-Byoung Chae, *Fellow, IEEE*, Kin-Fai Tong, *Fellow, IEEE*, and Yangyang Zhang

Abstract—This paper investigates the performance of a single-user fluid antenna system (FAS), by exploiting a class of elliptical copulas to describe the structure of dependency amongst the fluid antenna ports. By expressing Jakes' model in terms of the Gaussian copula, we consider two cases: (i) the general case, i.e., any arbitrary correlated fading distribution; and (ii) the specific case, i.e., correlated Nakagami- m fading. For both scenarios, we first derive analytical expressions for the cumulative distribution function (CDF) and probability density function (PDF) of the equivalent channel in terms of multivariate normal distribution. Then, we obtain the outage probability (OP) and the delay outage rate (DOR) to analyze the performance of the FAS. By employing the popular rank correlation coefficients such as Spearman's ρ and Kendall's τ , we measure the degree of dependency in correlated arbitrary fading channels and illustrate how the Gaussian copula can be accurately connected to Jakes' model in FAS without complicated mathematical analysis. Numerical results show that increasing the fluid antenna size provides lower OP and DOR, but the system performance saturates as the number of antenna ports increases. In addition, our results indicate that FAS provides better performance compared to conventional single-fixed antenna systems even when the size of fluid antenna is small.

Index Terms—Fluid antenna system, arbitrary fading, correlation, Gaussian copula, SISO, outage probability.

I. INTRODUCTION

Recent developments in diversity and spatial multiplexing techniques have led to massive multiple-input multiple-output (MIMO) being a key technology for the fifth-generation (5G) wireless communication systems, in which a large number

The work of K. Wong and K. Tong is supported by the Engineering and Physical Sciences Research Council (EPSRC) under Grant EP/W026813/1. For the purpose of open access, the authors will apply a Creative Commons Attribution (CC BY) licence to any Author Accepted Manuscript version arising. The work of López-Martínez was funded in part by Consejería de Transformación Económica, Industria, Conocimiento y Universidades of Junta de Andalucía, and in part by MCIN/AEI/10.13039/501100011033 through grants EMERGIA20 00297 and PID2020-118139RB-I00. The work of C.-B. Chae is supported by the Institute of Information and Communication Technology Promotion (IITP) grant funded by the Ministry of Science and ICT (MSIT), Korea (No. 2021-0-02208, No. 2021-0-00486).

F. R. Ghadi and F. Javier López-Martínez are with the Communications and Signal Processing Lab, Telecommunication Research Institute (TELMA), Universidad de Málaga, Málaga, 29010, Spain. F. J. López-Martínez is also with the Department of Signal Theory, Networking and Communications, University of Granada, 18071, Granada, Spain (e-mail: farshad@ic.uma.es, fjlm@ugr.es).

K. Wong and K. Tong are with the Department of Electronic and Electrical Engineering, University College London, London WC1E 6BT, United Kingdom. K. Wong is also with Yonsei Frontier Lab, Yonsei University, Seoul, 03722, Korea (e-mail: {kai-kit.wong, k.tong}@ucl.ac.uk).

C. B. Chae is with School of Integrated Technology, Yonsei University, Seoul, 03722, Korea (e-mail: cbchae@yonsei.ac.kr).

Y. Zhang is with Kuang-Chi Science Limited, Hong Kong SAR, China (e-mail: yangyang.zhang@kuang-chi.com).

Corresponding author: Kai-Kit Wong.

Digital Object Identifier 10.1109/XXX.2021.XXXXXXX

of antennas are equipped in the form of an antenna array at a base station [1]–[5]. Even though the large number of antennas at the base stations in massive MIMO systems greatly improves multiplexing gains in the spatial domain and scales up the network capacity, the same increment in the number of antennas at user equipment is not generally anticipated due to physical limitations of mobile devices even in high-frequency bands where the antenna size becomes smaller. To address this challenge, novel fluid antenna systems (FAS) have been recently introduced as an emerging technology that promises to achieve remarkable diversity gain in the small space of mobile devices in sixth-generation (6G) wireless networks [6], [7]. In fact, FAS refers to a system where the antenna has the ability to switch its location (i.e., ports) instantly in a small space. By doing so, FAS enables the mobile receiver's side to obtain spatial diversity without the physical limitations of half-wavelength antenna spacing. This idea was motivated by the recent advances in flexible antennas such as liquid metal antennas or ionized solutions as well as reconfigurable radio frequency (RF) pixel-like antennas, e.g., [8]–[10].

A. Related Works

Several contributions have been recently made to investigate the performance of FAS in various wireless communication scenarios. In [6], the authors derived analytical expressions of the probability density function (PDF) and the cumulative density function (CDF) for their proposed FAS under spatially-correlated Rayleigh fading channels, and then obtained the exact and approximated outage probability (OP) in integral-form and closed-form expressions, respectively. The authors in [11] recently derived an integral-form expression of the OP for a point-to-point (P2P) FAS under Nakagami- m fading channels. In addition, the lower bound of ergodic capacity for FAS under Rayleigh fading channels was derived in [12]. Moreover, the OP for large-scale cellular networks that utilize FAS was analyzed in [13]. Furthermore, in order to apply practical FAS to realistic wireless networks, the performance of multiuser communication systems exploiting fluid antennas was analyzed in [14]–[17]. Additionally, the authors in [18] proposed novel algorithms utilizing a combination of machine learning methods and analytical approximation to accurately select the best port with the maximum signal-to-noise ratio (SNR) in FAS when the system observes only a few ports. It is rightly accepted that the FAS performance highly depends on the spatial correlation between the fluid antenna ports. Nevertheless, it was demonstrated in [19] that most previous investigations may not accurately capture such a correlation. In this regard, the authors in [20] proposed an eigenvalue-based model to approximate the spatial correlation given by

Jakes' model, where they indicated that under such model, the FAS has limited performance gain as the number of ports grows. However, with all the aforementioned considerations, there are several momentous practical questions over the FAS to date: (i) What is the correlation structure that needs to be designed to be able to maximize the performance of FAS? (ii) How to build a tractable model that can work for any arbitrary correlation matrix and capture the case of Jakes' as an example? Therefore, a tractable statistical approach is required to gain more insight into these important issues.

B. Motivation and Contributions

As mentioned above, one of the most important challenges in channel modeling of FAS is to accurately characterize the spatial correlation between the fluid antenna ports – and desirably, without a prohibitive complexity. Although great efforts have been performed in this context, there is a lack of precise methods that can describe such inherent correlation. Specifically, generating the joint multivariate distributions of correlated channels in FAS is extremely demanding due to mathematical and statistical limitations. For this reason, most previous works applied either the traditional statistical methods or asymptotic formulations to describe the fading channel correlation between the fluid antenna ports. One flexible statistical procedure to overcome this issue is to adopt copula theory which has become popular recently in performance analysis of various wireless communication systems [21]–[31].

In general, copulas are functions that can: (i) Generate the joint multivariate distributions of two or more arbitrary random variables (RVs) by only knowing the marginal distributions; (ii) describe the negative/positive dependence structure between two or more arbitrary RVs beyond linear correlation. Exploiting such properties, the authors in [32] have recently analyzed the performance of FAS under arbitrary fading distributions, using the family of Archimedean copulas to derive the OP in a closed-form expression. However, this approach can only capture the impact of the number of fluid antenna ports on the OP performance, and cannot evaluate the effect of fluid antenna size on the FAS performance – which is a much more important parameter.

Motivated by the aforesaid observations, this paper proposes a novel copula-based technique to investigate the performance of FAS under arbitrary fading distributions. By expressing Jakes' model in terms of Gaussian copula¹ to describe the spatial correlation amongst the fluid antenna ports, we first study a general case that is valid for any arbitrary correlated fading distribution, and then analyze a specific case of correlated Nakagami- m fading channels. In both cases, we derive compact analytical expressions of the PDF and CDF for the considered FAS, exploiting Gaussian copula. Then, to evaluate the system performance, we obtain the analytical expressions of the OP and delay outage rate (DOR) for both cases. To gain more insight into the superiority of our copula-based approach,

¹The Gaussian copula is an elliptical and symmetric copula that is determined entirely by its correlation matrix, instead of a single parameter as with Archimedean copulas. In contrast to other copulas, the univariate margins in elliptical copula are joined by an elliptical distribution, which provides nice analytical properties [33].

we also measure the degree of dependence between correlated antenna ports. Specifically, the main contributions of our work are summarized as follows:

- We provide general formulations of the CDF, PDF, OP, and DOR in terms of the multivariate normal distribution for the considered FAS for any arbitrary fading distribution and also Jakes' model as an example.
- In addition, we quantify the structure of dependency between spatially correlated antenna ports by exploiting the important rank correlation coefficients such as Spearman's ρ and Kendall's τ , where the scatterplots for the 2-port FAS are provided for exemplary purposes.
- We derive the CDF, PDF, OP, and DOR in terms of the multivariate normal distribution under correlated Nakagami- m fading channels.
- Numerical results indicate that the Gaussian copula can accurately capture the spatial correlation between the fluid antenna ports in terms of the fluid antenna size and the number of ports. Furthermore, the results reveal that the performance of FAS highly depends on the fluid antenna size and the number of ports, namely, increasing the fluid antenna size improves the OP and DOR but the system performance does not necessarily get better as the number of ports grows.

C. Paper Organization

The rest of this paper is organized as follows. Section II describes the system model. Section III presents the performance analysis of the considered FAS so that the copula concept, general case analysis, and specific case analysis are provided in Subsections III-A, III-B, and IV-B, respectively. In Section V, the efficiency of analytical results is illustrated numerically, and finally, the conclusions are drawn in Section VI.

D. Mathematical Notation

We use boldface upper and lower case letters for matrices and column vectors, respectively. $\text{Cov}[\cdot]$ and $\text{Var}[\cdot]$ denote the covariance and variance operators, respectively. Moreover, $(\cdot)^T$, $(\cdot)^{-1}$, $|\cdot|$, and $\det(\cdot)$ stand for the transpose, inverse, magnitude, and determinant, respectively.

II. SYSTEM MODEL

We consider a wireless communication system as shown in Fig. 1, where a single-antenna transmitter sends an independent message x with transmit power P to a mobile receiver that is equipped with a fluid antenna. We assume that the fluid antenna includes only one RF chain and K preset positions (i.e., ports), which are equally distributed on a linear space of length $W\lambda$ where λ denotes the wavelength of the radiation. Therefore, the distance between the first port and the k -th port is given by

$$d_k = \left(\frac{k-1}{K-1} \right) W\lambda, \quad \text{for } k = 1, 2, \dots, K. \quad (1)$$

Furthermore, the received signal at the k -th port under flat fading condition can be expressed as

$$y_k = h_k x + z_k, \quad (2)$$

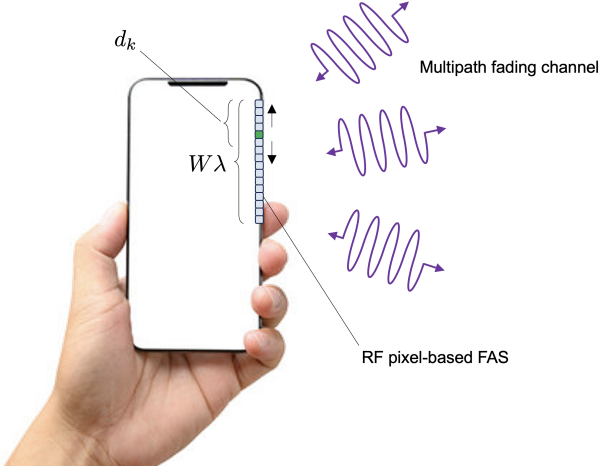


Fig. 1. Illustration of FAS.

in which h_k denotes the fading channel coefficient of the k -th port and z_k is the independent identically distributed (i.i.d.) additive white Gaussian noise (AWGN) with zero mean and variance σ_n^2 at every port.

Given that the fluid antenna ports can be arbitrarily close to each other, the fading channel coefficients $\{h_k\}_{\forall k}$ are spatially correlated and have a covariance matrix \mathbf{K} . Assuming 2-D isotropic scattering (i.e., rich scattering) and isotropic receiver ports on the FAS, such spatial correlation can be characterized by Jakes' model so that [34]

$$\mathbf{K}_{g_k, g_l} = \text{Cov}[h_k, h_l] = \sigma^2 J_0 \left(\frac{2\pi(k-l)}{K-1} W \right), \quad (3)$$

where σ^2 accounts for the large-scale fading effect and $J_0(\cdot)$ denotes the zero-order Bessel function of the first kind.

Moreover, in order to achieve optimal performance, FAS is assumed to always activate the best port with the maximum signal envelope for communication,² i.e.,

$$h_{\text{FAS}} = \max \{|h_1|, |h_2|, \dots, |h_K|\}. \quad (4)$$

Furthermore, the received SNR for the considered FAS can be defined as

$$\gamma = \frac{P h_{\text{FAS}}^2}{\sigma_n^2} = \bar{\gamma} h_{\text{FAS}}^2, \quad (5)$$

in which $\bar{\gamma} = \frac{P}{\sigma_n^2}$ is the average transmit SNR.

III. STATISTICAL CHARACTERIZATION

In this section, we first characterize the spatial correlation between the fluid antenna ports in terms of Gaussian copula, and then derive compact analytical expressions of the channel distributions for a general case. Next, we measure the structure of dependency for the FAS by exploiting rank correlation coefficients. To this end, we find it useful to first briefly review the concept of copula theory [35].

²In a practical scenario, only a small subset of observed ports is needed to reach the full channel state information (CSI) [18].

A. Brief Review of Copula Theory

Definition 1 (d -dimensional copula). Let $\mathbf{s} = [S_1, \dots, S_d]$ be a vector of d RVs with marginal CDFs $F_{S_i}(s_i)$ for $i \in \{1, 2, \dots, d\}$, respectively. Then, the corresponding joint CDF is defined as

$$F_{S_1, \dots, S_d}(s_1, s_2, \dots, s_d) = \Pr(S_1 \leq s_1, \dots, S_d \leq s_d). \quad (6)$$

The copula function $C(u_1, \dots, u_d)$ of the random vector \mathbf{s} defined on the unit hypercube $[0, 1]^d$ with uniformly distributed RVs $U_i := F_{S_i}(s_i)$ over $[0, 1]$ is given by

$$C(u_1, \dots, u_d) = \Pr(U_1 \leq u_1, \dots, U_d \leq u_d), \quad (7)$$

where $u_i = F_{S_i}(s_i)$.

Theorem 1 (Sklar's theorem). Let $F_{S_1, \dots, S_d}(s_1, \dots, s_d)$ be a joint CDF of RVs with margins $F_{S_i}(s_i)$ for $i \in \{1, 2, \dots, d\}$. Then, there exists one copula function C such that for all s_i in the extended real line domain $\bar{\mathbb{R}}$

$$F_{S_1, \dots, S_d}(s_1, \dots, s_d) = C(F_{S_1}(s_1), \dots, F_{S_d}(s_d)). \quad (8)$$

Definition 2 (d -dimension Gaussian copula). The multivariate Gaussian copula with correlation matrix $\mathbf{R} \in [-1, 1]^{d \times d}$ is defined as

$$C_G(u_1, \dots, u_d) = \Phi_{\mathbf{R}}(\phi^{-1}(u_1), \dots, \phi^{-1}(u_d); \eta), \quad (9)$$

where $\phi^{-1}(\cdot)$ is the inverse CDF (i.e., quantile function) of the standard normal distribution, $\Phi_{\mathbf{R}}(\cdot)$ is the joint CDF of the multivariate normal distribution with zero mean vector and correlation matrix \mathbf{R} , and η denotes the dependence parameter of the Gaussian copula which can control the degree of dependence between correlated RVs.

B. General Case: Arbitrary Correlated Fading Distribution

1) *Channel distributions*: By exploiting the concept of copula theory and using the definition of d -dimension Gaussian copula, we derive the compact analytical expressions of the CDF and PDF of h_{FAS} in the following theorems.

Theorem 2. The CDF of $h_{\text{FAS}} = \max \{|h_1|, |h_2|, \dots, |h_K|\}$ for any arbitrary correlated fading coefficient $|h_k|$, $k \in \{1, 2, \dots, K\}$, with marginal CDF $F_{|h_k|}(r)$ by exploiting Gaussian copula is derived as

$$F_{h_{\text{FAS}}}(r) = \Phi_{\mathbf{R}_{h_k, h_l}}(\phi^{-1}(F_{|h_1|}(r)), \dots, \phi^{-1}(F_{|h_K|}(r))), \quad (10)$$

where

$$\phi^{-1}(F_{|h_K|}(r)) = \sqrt{2} \text{erf}^{-1}(2F_{|h_K|}(r) - 1), \quad (11)$$

in which $\text{erf}^{-1}(\cdot)$ denotes the inverse of error function $\text{erf}(z) = \frac{2}{\sqrt{\pi}} \int_0^z e^{-t^2} dt$. The term $\Phi_{\mathbf{R}_{h_k, h_l}}(\cdot)$ is the joint CDF of the multivariate normal distribution with zero mean vector and the correlation matrix \mathbf{R}_{h_k, h_l} as

$$\mathbf{R}_{h_k, h_l} = \begin{bmatrix} 1 & \eta_{1,2} & \dots & \eta_{1,l} \\ \eta_{2,1} & 1 & \dots & \eta_{2,l} \\ \vdots & \vdots & \ddots & \vdots \\ \eta_{k,1} & \eta_{k,2} & \dots & 1 \end{bmatrix}, \quad (12)$$

where $\eta_{k,l} = J_0\left(\frac{2\pi(k-l)W}{K-1}\right)$ is the dependence parameter of Gaussian copula which can be chosen freely to control the correlation between the corresponding channel coefficients.

Proof. Since the structure of dependency between correlated RVs in the Gaussian copula is denoted by a correlation matrix with corresponding dependence parameters, we first determine the correlation matrix between the arbitrary channel coefficients in terms of Jakes' model. Hence, by exploiting the covariance matrix in (3) and considering Cholesky decomposition, the correlation matrix \mathbf{R}_{h_k, h_l} includes dependence parameter $\eta_{k,l}$ is obtained as

$$\mathbf{R}_{h_k, h_l} = \frac{\text{Cov}[h_k, h_l]}{\sqrt{\text{Var}[h_k] \text{Var}[h_l]}} = J_0\left(\frac{2\pi(k-l)W}{K-1}\right). \quad (13)$$

Next, by using the definition of the CDF, $F_{h_{\text{FAS}}}(r)$ can be mathematically expressed as

$$F_{h_{\text{FAS}}}(r) = \Pr(\max\{|h_1|, |h_2|, \dots, |h_K|\} \leq r) \quad (14)$$

$$= \Pr(|h_1| \leq r, |h_2| \leq r, \dots, |h_K| \leq r) \quad (15)$$

$$= F_{|h_1|, |h_2|, \dots, |h_K|}(r, r, \dots, r) \quad (16)$$

$$\stackrel{(a)}{=} C(F_{|h_1|}(r), F_{|h_2|}(r), \dots, F_{|h_K|}(r)), \quad (17)$$

where (a) is obtained from Theorem 1. Now, by inserting the Gaussian copula from (9) into (14), then plugging the marginal CDF of arbitrary fading channels into the obtained result for $u_d = F_{|h_k|}(r)$, and finally considering the correlation matrix in (13), the proof is completed. ■

Theorem 3. The PDF of $h_{\text{FAS}} = \max\{|h_1|, |h_2|, \dots, |h_K|\}$ for any arbitrary correlated fading coefficient $|h_k|$, for $k \in \{1, 2, \dots, K\}$, with marginal PDF $f_{|h_k|}(r)$ and marginal CDF $F_{|h_k|}(r)$ by exploiting Gaussian copula is derived as

$$f_{h_{\text{FAS}}}(r) = \prod_{k=1}^K f_{|h_k|}(r) \times \frac{\exp\left(-\frac{1}{2}(\phi_{h_K}^{-1})^T (\mathbf{R}_{h_k, h_l}^{-1} - \mathbf{I}) \phi_{h_K}^{-1}\right)}{\sqrt{\det(\mathbf{R}_{h_k, h_l})}}, \quad (18)$$

where $\det(\mathbf{R}_{h_k, h_l})$ denotes the determinant of the correlation matrix \mathbf{R}_{h_k, h_l} , \mathbf{I} is the identity matrix, and $\phi_{h_K}^{-1} = [\phi^{-1}(F_{|h_1|}(r)), \dots, \phi^{-1}(F_{|h_K|}(r))]^T$ is given by (11).

Proof. By applying the chain rule to $F_{h_{\text{FAS}}}(r)$ provided in (10), and then considering the marginal distributions of arbitrary fading channels, we have

$$f_{h_{\text{FAS}}}(r) = \prod_{k=1}^K f_{|h_k|}(r) \times \underbrace{\frac{\partial^K \Phi_{\mathbf{R}_{h_k, h_l}}(\phi^{-1}(F_{|h_1|}(r)), \dots, \phi^{-1}(F_{|h_K|}(r)))}{\partial F_{|h_1|}(r) \dots \partial F_{|h_K|}(r)}}_{c_G(F_{|h_1|}(r), \dots, F_{|h_K|}(r))}, \quad (19)$$

where $c_G(F_{|h_1|}(r), \dots, F_{|h_K|}(r))$ is the Gaussian copula density which can be computed mathematically as

$$c_G(F_{|h_1|}(r), \dots, F_{|h_K|}(r)) = \frac{\exp\left(-\frac{1}{2}(\phi_{h_K}^{-1})^T (\mathbf{R}_{h_k, h_l}^{-1} - \mathbf{I}) \phi_{h_K}^{-1}\right)}{\sqrt{\det(\mathbf{R}_{h_k, h_l})}}. \quad (20)$$

Now, by inserting (20) into (19) and considering the correlation matrix \mathbf{R}_{h_k, h_l} , the proof is completed. ■

2) Dependence measurement: In order to gain more insight into how our copula-based analytical results can describe the structure of dependency between correlated fading channel coefficients over the fluid antenna ports, we here provide the scatterplots of two arbitrarily correlated fading channels $|h_1|$ and $|h_2|$ by using Gaussian copula over the 2-port FAS in Fig. 2. To do so, by considering uniformly distributed RVs $u_1 = F_{|h_1|}(|h_1|)$ and $u_2 = F_{|h_2|}(|h_2|)$, we generate $n = 1000$ random vectors from the Gaussian copula $C_G(u_1, u_2)$ with correlation matrix \mathbf{R}_{h_1, h_2} consisting of two dependence parameters $\eta_{1,2}$ and $\eta_{2,1}$. Given that we considered Jakes' model to describe the spatial correlation between the fluid antenna ports, both dependence parameters highly depend on the fluid antenna size W . Thus, we can observe from Fig. 2 that as the size of the fluid antenna increases (decreases), the scattering between data generated by the Gaussian copula increases (decreases), meaning that the spatial correlation between the fluid antenna ports becomes weaker (stronger). Furthermore, these observations are completely separate from the marginal distributions of channel coefficients, which means that $|h_1|$ and $|h_2|$ can be modeled by any arbitrary marginal distributions whereas they still have the same correlation. However, to realize the spatial correlation between the fluid antenna ports under specific channel distributions, we just need to apply the inverse CDF of the corresponding distribution to the uniformly distributed RVs u_1 and u_2 (i.e., $|h_1| = F_{|h_1|}^{-1}(u_1)$ and $|h_2| = F_{|h_2|}^{-1}(u_2)$), in which the spatial correlation for a specific scenario will be analyzed in the next section.

On the other hand, it should be noted that the dependence parameter of Gaussian copula η in Def. 2 does not necessarily express the linear correlation between two or more RVs, since when non-linear transformations are applied to those RVs, the linear correlation cannot be maintained anymore (as it happens in the copula definition). For this reason, a rank correlation that can measure the statistical dependence between the *ranking* of two RVs is often used to describe the correlation between RVs. In other words, unlike the linear correlation coefficient which can only describe linear dependence between RVs, rank correlations are preserved under any monotonic transformation, and thus can significantly describe the non-linear correlation between RVs. In this regard, Spearman's ρ , denoted as ρ_s , and Kendall's τ , denoted as τ_k , are the two most popular rank correlation coefficients which can accurately describe such dependence between RVs since they are invariant to the choice of the marginal distribution. Additionally, ρ_s and τ_k for the

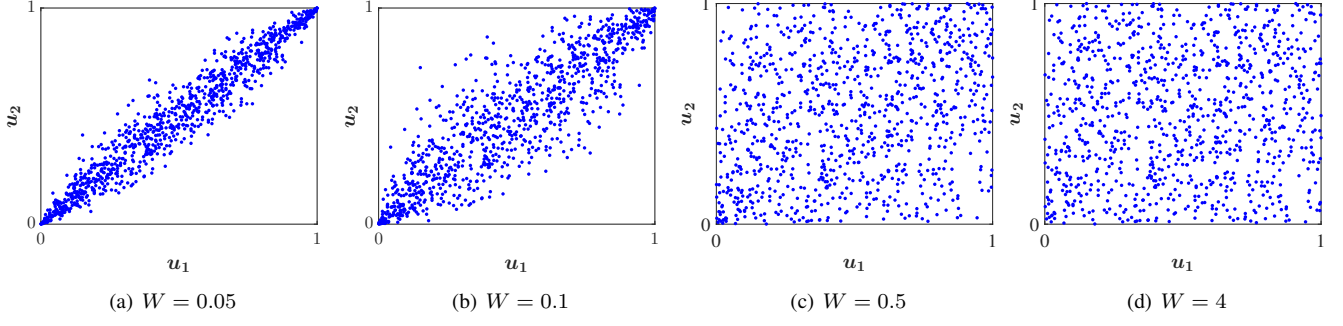


Fig. 2. Scatterplots describe the structure of dependency between two arbitrary correlated fading channels $|h_1|$ and $|h_2|$ with uniform marginal distributions u_1 and u_2 under Gaussian copula that includes correlation matrix \mathbf{R}_{h_1, h_2} .

TABLE I
DEPENDENCE MEASUREMENT IN TERMS OF THE FLUID ANTENNA SIZE W
FOR THE CONSIDERED FAS WHEN $K = 2$

Dependence measurement for a 2-port FAS						
Size W	$\eta_{1,2}$	$\eta_{2,1}$	$\rho_{s1,2}$	$\rho_{s2,1}$	$\tau_{k1,2}$	$\tau_{k2,1}$
$W = 0.05$	0.98	0.98	0.97	0.97	0.86	0.86
$W = 0.1$	0.90	0.90	0.89	0.89	0.72	0.72
$W = 0.5$	0.30	0.30	0.29	0.29	0.20	0.20
$W = 1$	0.22	0.22	0.21	0.21	0.14	0.14
$W = 2$	0.16	0.16	0.15	0.15	0.10	0.10
$W = 4$	0.11	0.11	0.10	0.10	0.07	0.07
$W = 6$	0.09	0.09	0.09	0.09	0.06	0.06

two arbitrary RVs with the corresponding copula C can be expressed, respectively, as [35]

$$\rho_s = 12 \iint_{[0,1]^2} u_1 u_2 dC(u_1, u_2) - 3, \quad (21)$$

$$\tau_k = 4 \iint_{[0,1]^2} C(u_1, u_2) dC(u_1, u_2) - 1. \quad (22)$$

In particular, for the two arbitrary correlated fading channel coefficients $|h_1|$ and $|h_2|$ with the Gaussian copula C_G , which is defined in terms of bivariate normal distribution, $\rho_{s_{k,l}}$ and $\tau_{k_{k,l}}$ can be, respectively, expressed in terms of $\eta_{k,l}$ as

$$\rho_{s_{k,l}} = \frac{6}{\pi} \arcsin\left(\frac{\eta_{k,l}}{2}\right), \quad (23)$$

$$\tau_{k_{k,l}} = \frac{2}{\pi} \arcsin(\eta_{k,l}). \quad (24)$$

Therefore, by inserting the correlation matrix \mathbf{R}_{h_k, h_l} from (13) which depends on the fluid antenna size W into (24) and (23), we provide the dependence measurement between two arbitrary correlated channel coefficients $|h_1|$ and $|h_2|$ over the FAS in terms of the rank correlations $\rho_{s_{k,l}}$ and $\tau_{k_{k,l}}$ in Tab. I. It is worth noting that the rank correlation coefficients are strictly less than the Gaussian dependence parameter unless $\eta_{k,l}$ is exactly one (i.e., the perfect correlation).

IV. PERFORMANCE ANALYSIS

Here, we first derive compact analytical expressions of the OP and DOR for a general case. Then in order to evaluate the FAS performance, we obtain the OP and DOR under correlated Nakagami- m fading channels as a special case.

A. General Case: Arbitrary Correlated Fading Distribution

1) *OP analysis*: OP is a key performance metric in wireless communication systems which is defined as the probability that the random SNR γ is less than an SNR threshold γ_{th} , i.e., $P_{out} = \Pr(\gamma \leq \gamma_{th})$. Hence, we derive the OP for the considered FAS in the following theorem.

Theorem 4. *The OP for the considered FAS under arbitrary correlated fading channels by exploiting Gaussian copula is given by*

$$P_{out} = \Phi_{\mathbf{R}_{h_k, h_l}}(\phi^{-1}(F_{|h_1|}(\hat{\gamma})), \dots, \phi^{-1}(F_{|h_K|}(\hat{\gamma}))), \quad (25)$$

in which $\phi^{-1}(F_{|h_K|}(\hat{\gamma})) = \sqrt{2} \text{erf}^{-1}(2F_{|h_K|}(\hat{\gamma}) - 1)$, $\hat{\gamma} = \sqrt{\frac{\gamma_{th}}{\gamma}}$, and the correlation matrix \mathbf{R}_{h_k, h_l} is defined in (12).

Proof. By substituting the SNR of the FAS from (5) into the definition of OP, we have

$$P_{out} = \Pr\left(\max\{|h_1|, \dots, |h_K|\} \leq \sqrt{\frac{\gamma_{th}}{\gamma}}\right) = F_{h_{FAS}}(\hat{\gamma}), \quad (26)$$

where by utilizing the CDF in (10), the proof is completed. ■

2) *DOR analysis*: DOR is an important performance metric for designing ultra-reliable and low-latency communications (URLLC), which is defined as the probability that the time required to successfully transmit a certain amount of data R in a wireless channel with a bandwidth B is greater than a threshold duration T_{th} , i.e., $\Pr(T_{dt} > T_{th})$, where

$$T_{dt} = \frac{R}{B \log_2(1 + \gamma)} \quad (27)$$

represents the delivery time [36]. Hence, the DOR for the considered FAS can be derived in the following theorem.

Theorem 5. *The DOR for the considered FAS under arbitrary correlated fading channels by exploiting Gaussian copula is given by*

$$P_{dor} = \Phi_{\mathbf{R}_{h_k, h_l}}(\phi^{-1}(F_{|h_1|}(\hat{T})), \dots, \phi^{-1}(F_{|h_K|}(\hat{T}))), \quad (28)$$

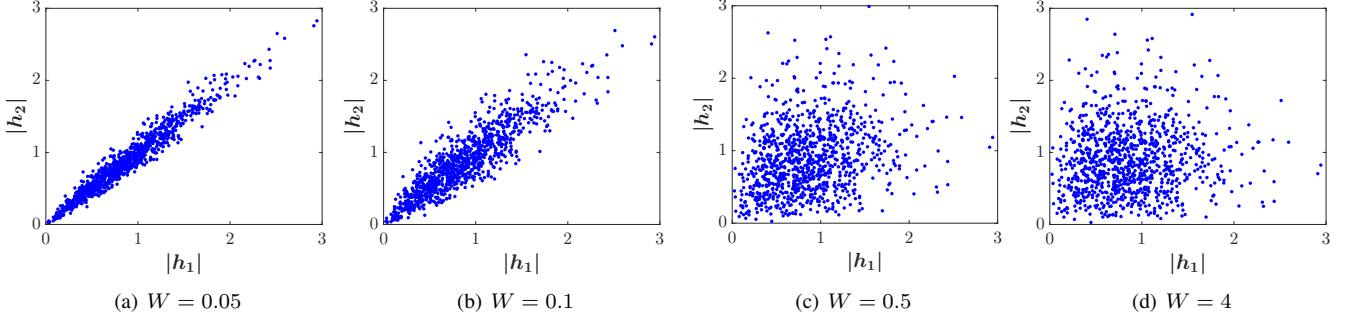


Fig. 3. Scatterplots describe the structure of dependency between two correlated Nakagami- m fading channels $|h_1|$ and $|h_2|$ when $m = 1$ under Gaussian copula that includes correlation matrix \mathbf{R}_{h_1, h_2} .

where $\phi^{-1}\left(F_{|h_K|}(\hat{T})\right) = \sqrt{2} \operatorname{erf}^{-1}\left(2F_{|h_K|}(\hat{T}) - 1\right)$, $\hat{T} = \sqrt{\frac{R \ln 2}{e^{\frac{R \ln 2}{BT_{th}}}}}$, and \mathbf{R}_{h_k, h_l} is obtained from (12).

Proof. By applying the SNR of the FAS to the definition of the DOR, we have

$$P_{\text{dor}} = \Pr\left(\frac{R}{B \log_2(1 + \gamma)} > T_{\text{th}}\right) \quad (29)$$

$$= \Pr\left(\gamma \leq \exp\left(\frac{R \ln 2}{BT_{\text{th}}}\right) - 1\right) \quad (30)$$

$$= \Pr\left(h_{\text{FAS}} \leq \sqrt{\frac{R \ln 2}{e^{\frac{R \ln 2}{BT_{\text{th}}}} - 1}}\right) \quad (31)$$

$$= F_{\text{FAS}}(\hat{T}), \quad (32)$$

which after using (10), completes the proof. ■

Remark 1. It is worth noting that the obtained analytical results in Thms. 2, 3, 4, 5 are valid for any choice of arbitrary correlated fading distributions. Though these analytical results, except the PDF, are expressed in terms of the CDF of multivariate normal distributions, they can be estimated numerically by adopting different methods [37]–[39] and there is no need to solve any complicated integral to derive them. Additionally, in contrast to [32] which did not consider the size of the fluid antenna for describing the channel correlation, we can see that our copula-based analytical results can accurately describe the spatial correlation between the fluid antenna ports in terms of Jakes' model, and hence, we can consider the fluid antenna size in the performance analysis of the FAS.

B. Special Case: Correlated Nakagami- m Fading

To analyze the efficiency of the considered FAS in terms of the OP and DOR under typical fading conditions, we here consider that the channel coefficients follow Nakagami- m distribution, where the parameter $m \geq 0.5$ describes the fading severity and it can be reduced to Rayleigh distribution when $m = 1$. Therefore, the marginal PDF and CDF of the

fading channel coefficient $|h_k|$ with the shape parameter m and the spread parameter μ can be, respectively, written as

$$f_{|h_k|}^{\text{Nak}}(r) = \frac{2m^m}{\Gamma(m)\mu^m} r^{2m-1} e^{-\frac{m}{\mu} r^2}, \quad (33)$$

$$F_{|h_k|}^{\text{Nak}}(r) = \frac{\gamma\left(m, \frac{m}{\mu} r^2\right)}{\Gamma(m)}, \quad (34)$$

in which the terms $\Gamma(\cdot)$ and $\gamma(\cdot, \cdot)$ are gamma function and the lower incomplete gamma function, respectively.

Corollary 1. The CDF of $h_{\text{FAS}} = \max\{|h_1|, |h_2|, \dots, |h_K|\}$ under correlated Nakagami- m fading coefficient $|h_k|$, for $k \in \{1, 2, \dots, K\}$, with marginal CDF $F_{|h_k|}^{\text{Nak}}(r)$ by utilizing Gaussian copula is derived as

$$F_{h_{\text{FAS}}}^{\text{Nak}}(r) = \Phi_{\mathbf{R}_{h_k, h_l}}\left(\sqrt{2} \operatorname{erf}^{-1}\left(\frac{2\gamma\left(m, \frac{m}{\mu} r^2\right)}{\Gamma(m)} - 1\right), \dots, \sqrt{2} \operatorname{erf}^{-1}\left(\frac{2\gamma\left(m, \frac{m}{\mu} r^2\right)}{\Gamma(m)} - 1\right)\right). \quad (35)$$

Proof. By inserting (34) into (11) and plugging the obtained result into (10), the proof is completed. ■

Corollary 2. The PDF of $h_{\text{FAS}} = \max\{|h_1|, |h_2|, \dots, |h_K|\}$ under correlated Nakagami- m fading coefficient $|h_k|$, for $k \in \{1, 2, \dots, K\}$, with marginal PDF $f_{|h_k|}^{\text{Nak}}(r)$ and marginal CDF $F_{|h_k|}^{\text{Nak}}(r)$ by exploiting Gaussian copula is derived as

$$f_{h_{\text{FAS}}}^{\text{Nak}}(r) = \frac{\left(\frac{2m^m}{\Gamma(m)\mu^m} r^{2m-1} e^{-\frac{m}{\mu} r^2}\right)^K}{\sqrt{\det(\mathbf{R}_{h_k, h_l})}} \times \exp\left(-\frac{1}{2} \left(\boldsymbol{\phi}_{h_K}^{\text{Nak}-1}\right)^T \left(\mathbf{R}_{h_k, h_l}^{-1} - \mathbf{I}\right) \boldsymbol{\phi}_{h_K}^{\text{Nak}-1}\right), \quad (36)$$

where

$$\boldsymbol{\phi}_{h_K}^{\text{Nak}-1} = \left[\sqrt{2} \operatorname{erf}^{-1}\left(\frac{2\gamma\left(m, \frac{m}{\mu} r^2\right)}{\Gamma(m)} - 1\right), \dots, \sqrt{2} \operatorname{erf}^{-1}\left(\frac{2\gamma\left(m, \frac{m}{\mu} r^2\right)}{\Gamma(m)} - 1\right)\right]. \quad (37)$$

Proof. By substituting the marginal distribution of the Nakagami- m channel $|h_K|$ from (33) and (34) into (18) and considering the correlation in (12), the proof is completed. ■

Remark 2. It is worth mentioning that the spatial correlation between correlated Nakagami- m fading coefficients $|h_1|$ and $|h_2|$ under Gaussian copula can be measured by applying the inverse CDF of Nakagami- m to the uniformly distributed RVs u_1 and u_2 (i.e., $|h_1| = F_{|h_1|}^{\text{Nak}^{-1}}(u_1)$ and $|h_2| = F_{|h_2|}^{\text{Nak}^{-1}}(u_2)$). Following this approach, Fig. 3 shows the scatterplots of fading coefficients $|h_1|$ and $|h_2|$ under Nakagami- m fading, where it confirms that for small (large) fluid antenna size W , the fading channel coefficients are highly (slightly) correlated.

Remark 3. By plotting the CDF of FAS from (35) in Fig. 4, we can see that as K changes from 4 to 8 for small values of W , the CDF remains almost constant, which means that the FAS performance does not necessarily improve as K grows. However, for large values of W the CDF remarkably shifts to the right as K increases, i.e., the performance improves. In addition, we observe that as W grows for a fixed value of K (e.g., $K = 8$), the CDF significantly shifts to the right, meaning that for constant K , increasing the fluid antenna size improves considerably the FAS performance.

Corollary 3. The OP for the considered FAS under correlated Nakagami- m fading channels by exploiting Gaussian copula is given by

$$P_{\text{out}}^{\text{Nak}} = \Phi_{\mathbf{R}_{h_k, h_l}} \left(\sqrt{2} \operatorname{erf}^{-1} \left(\frac{2\gamma \left(m, \frac{m}{\mu} \hat{\gamma}^2 \right)}{\Gamma(m)} - 1 \right), \dots, \sqrt{2} \operatorname{erf}^{-1} \left(\frac{2\gamma \left(m, \frac{m}{\mu} \hat{\gamma}^2 \right)}{\Gamma(m)} - 1 \right) \right). \quad (38)$$

Proof. By assuming $r = \hat{\gamma}$ in (35), the proof is completed. ■

Corollary 4. The DOR for the considered FAS under correlated Nakagami- m fading channels by exploiting Gaussian copula is given by

$$P_{\text{dor}}^{\text{Nak}} = \Phi_{\mathbf{R}_{h_k, h_l}} \left(\sqrt{2} \operatorname{erf}^{-1} \left(\frac{2\gamma \left(m, \frac{m}{\mu} \hat{T}^2 \right)}{\Gamma(m)} - 1 \right), \dots, \sqrt{2} \operatorname{erf}^{-1} \left(\frac{2\gamma \left(m, \frac{m}{\mu} \hat{T}^2 \right)}{\Gamma(m)} - 1 \right) \right). \quad (39)$$

Proof. By assuming $r = \hat{T}$ in (35), the proof is done. ■

V. NUMERICAL RESULTS

In this section, we present numerical results to gain more insight into the performance of considered FAS in terms of the OP and the DOR. It should be noted that the analytical results obtained in (38) and (39) are expressed in terms of the CDF of a multivariate normal distribution that technically has no closed-form expression. Nonetheless, it can be estimated numerically through various algorithms or implemented by

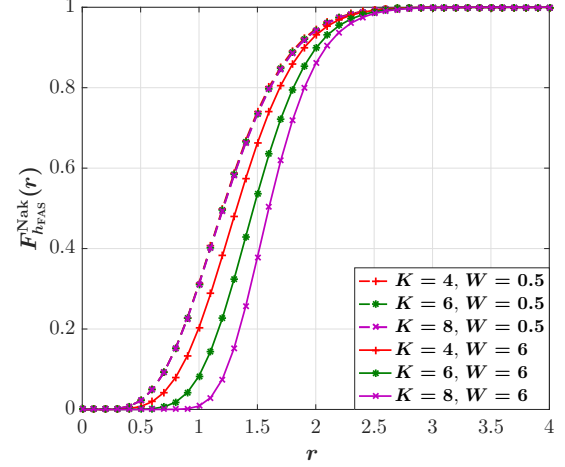


Fig. 4. CDF of FAS for selected values of K and W when $\mu = 1$.

the mathematical package of programming languages such as MATLAB, Python, and R. Additionally, as shown in Algorithm 1, the Gaussian copula can be simulated by applying the Cholesky decomposition of the given correlation matrix \mathbf{R} to obtain the lower triangular matrix \mathbf{A} , such that $\mathbf{A}\mathbf{A}^T = \mathbf{R}$ [40]. We also consider the conventional single-input single-output (SISO) fixed-antenna system as a benchmark to compare with the proposed FAS.

Algorithm 1 Gaussian Copula Simulation

Step 1. Compute \mathbf{A} , such that $\mathbf{A}\mathbf{A}^T = \mathbf{R}$
Step 2. Generate $\mathbf{s} = (S_1, \dots, S_d)$, such that $S_i \sim \mathcal{N}(0, 1)$ for $i = 1, \dots, d$
Step 3. Calculate $V_i = \sum_{j=1}^d A_{i,j} S_j$ for $i = 1, \dots, d$
Step 4. Return $U_i = \Phi_{\mathbf{R}}(V_i)$ for $i = 1, \dots, d$

The behavior of the OP and DOR versus the average transmit SNR $\bar{\gamma}$ for given numbers of fluid antenna ports K and selected values of fluid antenna size W under correlated Nakagami- m fading channels is illustrated in Figs. 5 and 6, respectively. As expected, we can see that the OP and DOR rise as the average transmit SNR increases. From Figs. 5(a) and 6(a), it can also be observed that as K grows, the performance of OP and DOR improves for large values of fluid antenna size (e.g., $W = 6$) which is in alignment with the findings of [20]. However, increasing K does not affect the system performance for small values of fluid antenna size (e.g., $W = 0.5$), meaning that the OP and DOR remain almost constant. In other words, when K rises for a fixed W , the space between ports decreases and the spatial correlation between them increases, and thus lower diversity gain is reached until eventually saturating. Furthermore, we can observe from Figs. 5(b) and 6(b) that increasing the fluid antenna size W for larger K provides more noticeable effects on the improvement of OP and DOR compared with smaller K . Moreover, it can be seen that increasing the spatial separation between the fluid antenna ports by increasing W for a fixed K , and hence reducing the spatial correlation, can greatly ameliorate the system performance in terms of the OP

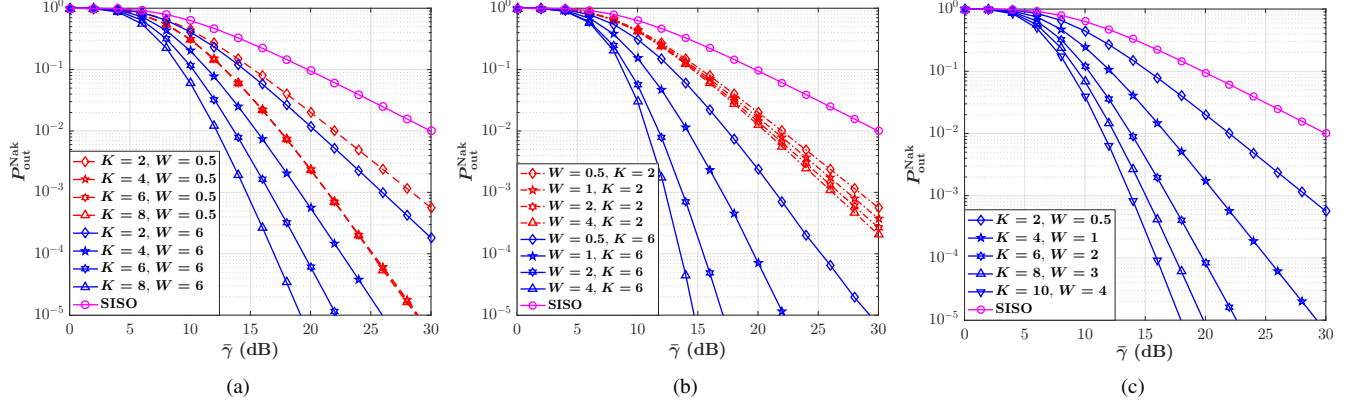


Fig. 5. OP versus average transmit SNR $\bar{\gamma}$ for selected values of W and K when $\gamma_{th} = 10\text{dB}$, $m = 1$, and $\mu = 1$.

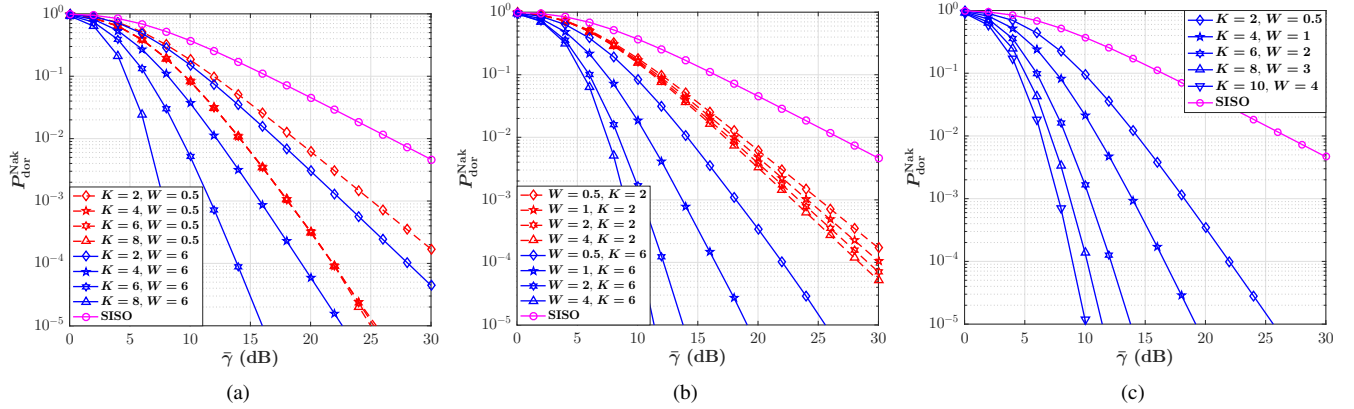


Fig. 6. DOR versus average transmit SNR $\bar{\gamma}$ for selected values of W and K when $\gamma_{th} = 10\text{dB}$, $B = 2\text{MHz}$, $R = 5\text{Kbits}$, $T_{th} = 3\text{ms}$, $m = 1$, and $\mu = 1$.

and DOR. Figs. 5(c) and 6(c) indicate that by simultaneously increasing W and K , spatial correlation between fluid antenna ports becomes balanced, and consequently lower OP and DOR are achieved. Besides, it can be seen that the FAS provides better performance in terms of the OP and DOR compared with the conventional SISO system in all scenarios even if the fluid antenna has large K and small space. The main reason behind this improvement is due the capability of FAS in switching to the best port within a finite size W .

The impact of fading parameter m on the performance of OP and DOR for given values of K and W under correlated Nakagami- m fading channels is presented in Figs. 7(a) and 7(b), respectively. It is clearly seen that the efficiency of the OP and DOR improves under a mild fading condition (e.g., $m = 3$) than when a stronger one (e.g., $m = 0.5$) is considered, especially when the average SNR $\bar{\gamma}$ grows. Regarding the importance of fluid antenna size W in the design of FAS in realistic scenarios, we evaluate the behavior of the OP and DOR in terms of W for different values of $\bar{\gamma}$ in Figs. 8(a) and 8(a), respectively. As expected, increasing the spatial separation between the fluid antenna ports for a fixed K can provide lower values of the OP and DOR. We can also see that even under small values of $\bar{\gamma}$ and W such as 0.5, FAS offers better performance than the SISO

system.

Fig. 9(a) shows the DOR performance against the amount of transmitted data R for different values of W and K in FAS. As expected, we can see that the DOR performance becomes worse as R increases. Nonetheless, increasing the number of fluid antenna ports as well as the fluid antenna size can lead to reaching a lower DOR when a fixed amount of data is sent. For instance, sending $R = 6\text{Kbits}$ amounts of data becomes almost impossible with low delay when W and K are small or when the SISO system is considered, but it can be transmitted with small delay if FAS is considered with large values of W and K . The impact of bandwidth B variations on the DOR performance for the considered FAS is illustrated in Fig. 9(b). It is obvious that the preset amounts of data can be sent with a lower delay when the channel bandwidth increases. Additionally, it can be seen that for a fixed B , the DOR performance significantly improves as W and K increase, meaning that data can be transmitted with a lower delay in FAS compared with the SISO system.

VI. CONCLUSIONS

In this paper, we studied the performance of FAS under arbitrary correlated fading channel coefficients, in which we exploited copula theory to describe the dependence structure

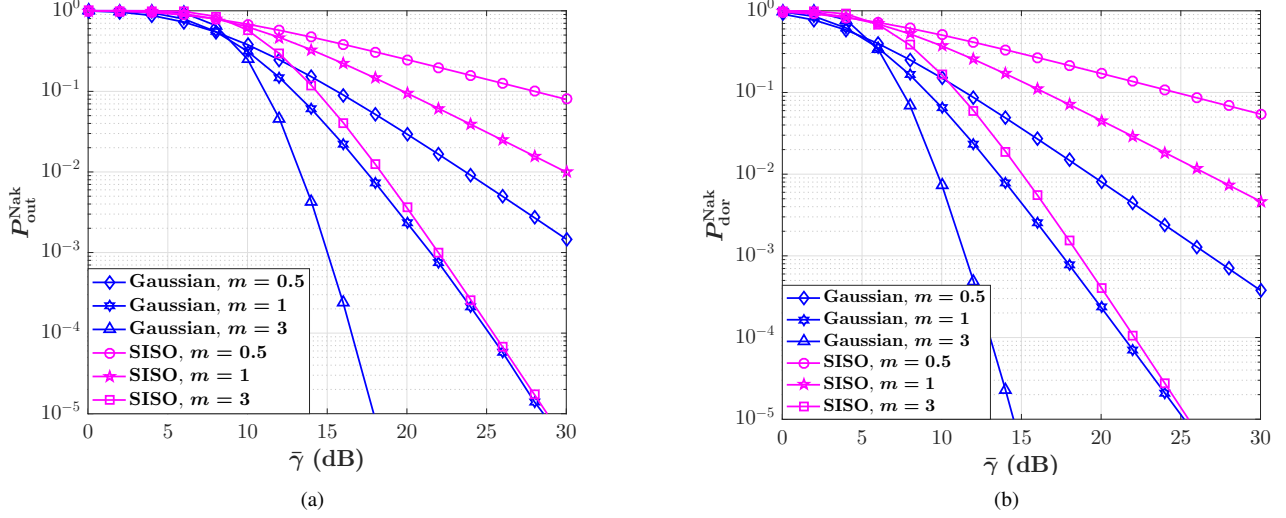


Fig. 7. (a) OP and (b) DOR versus average transmit SNR $\bar{\gamma}$ for selected values of fading parameter m when $\gamma_{th} = 10\text{dB}$, $K = 3$, $W = 2.5$, $B = 2\text{MHz}$, $R = 5\text{Kbits}$, $T_{th} = 3\text{ms}$, and $\mu = 1$.

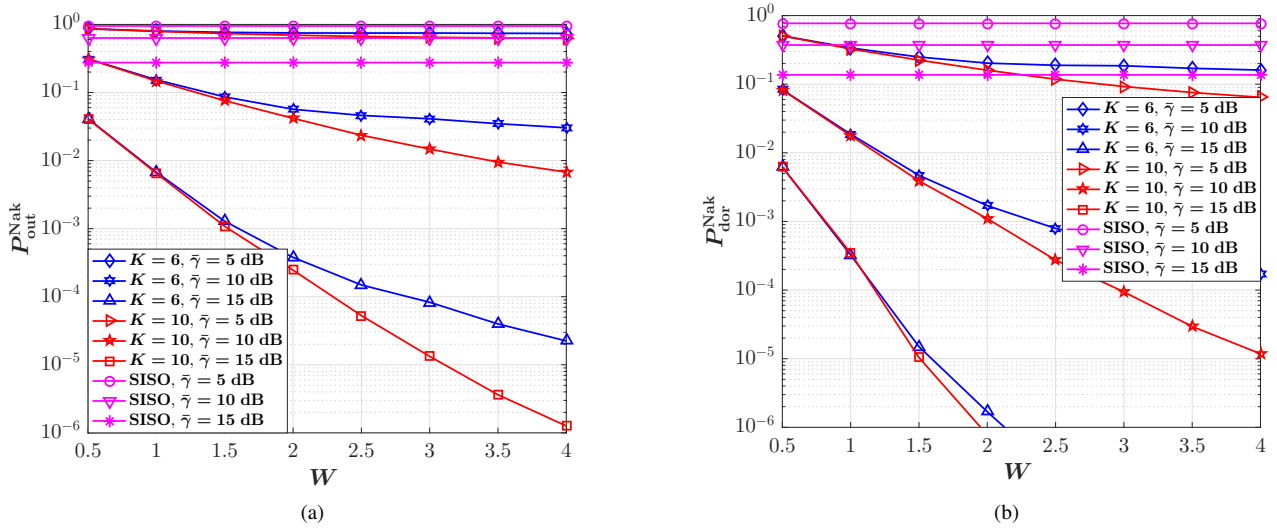


Fig. 8. (a) OP and (b) DOR versus fluid antenna size W for selected values of fading parameter K and $\bar{\gamma}$ when $\gamma_{th} = 10\text{dB}$, $B = 2\text{MHz}$, $R = 5\text{Kbits}$, $T_{th} = 3\text{ms}$, and $\mu = 1$.

between the fluid antenna ports. To this end, we first expressed Jakes' model in terms of Gaussian copula and then we derived compact analytical expressions for the CDF, PDF, OP, and DOR in terms of multivariate normal distribution for a general case, which are valid for any arbitrary choice of fading distribution. Next, we quantified the spatial correlation between the fluid antenna ports with the help of popular rank correlation coefficients (i.e., Spearman's ρ and Kendall's τ) and indicated the accuracy of using Gaussian copula in FAS. Furthermore, to analyze the system performance in typical scenarios, we obtained analytical expressions of the CDF, PDF, OP, and DOR under correlated Nakagami- m fading channels. Numerical results indicated that the system performance highly depends on the antenna size and the number of ports, so increasing the fluid antenna size provides lower OP and DOR but increasing

the number of fluid antenna ports does not necessarily offer a better performance.

REFERENCES

- [1] L. Zheng and D. N. C. Tse, "Diversity and multiplexing: A fundamental tradeoff in multiple-antenna channels," *IEEE Trans. Inf. Theory*, vol. 49, no. 5, pp. 1073–1096, 2003.
- [2] P. Von Butovitsch, D. Astely, C. Friberg, A. Furuskär, B. Göransson, B. Hogan, J. Karlsson, and E. Larsson, "Advanced antenna systems for 5G networks," *Ericsson white paper*, 2018.
- [3] E. G. Larsson, O. Edfors, F. Tufvesson, and T. L. Marzetta, "Massive MIMO for next generation wireless systems," *IEEE Commun. Mag.*, vol. 52, no. 2, pp. 186–195, 2014.
- [4] J. Zhang, S. Chen, Y. Lin, J. Zheng, B. Ai, and L. Hanzo, "Cell-free massive MIMO: A new next-generation paradigm," *IEEE Access*, vol. 7, pp. 99 878–99 888, 2019.
- [5] T. L. Marzetta, "Massive MIMO: an introduction," *Bell Syst. Tech. J.*, vol. 20, pp. 11–22, 2015.

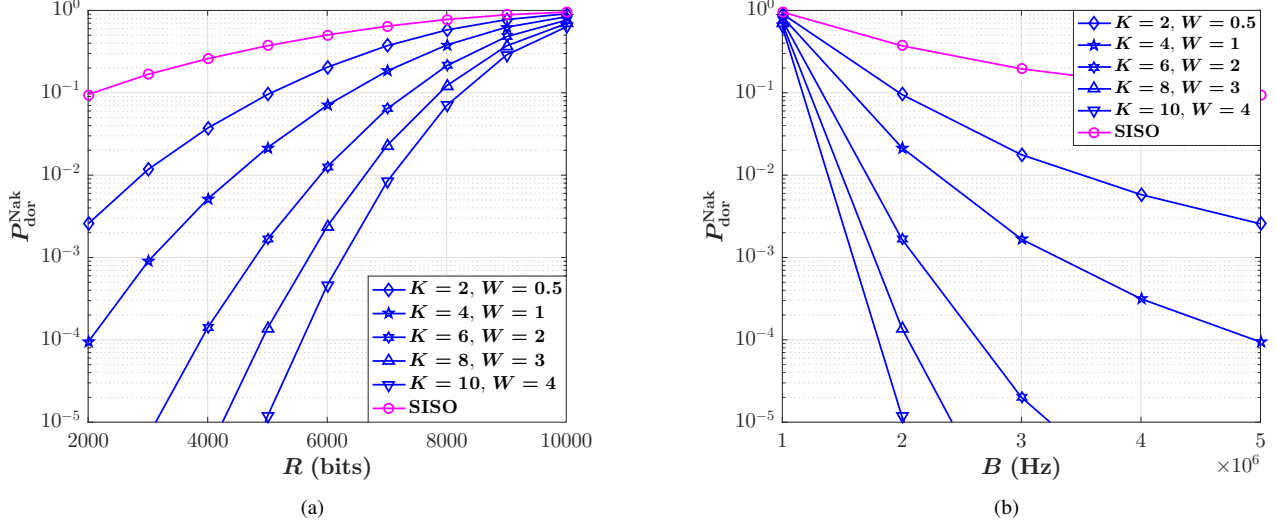


Fig. 9. (a) DOR versus amount of data R and (b) DOR versus bandwidth B for selected values of fading parameter K and $\bar{\gamma}$ when $\gamma_{th} = 10\text{dB}$, $B = 2\text{MHz}$, $R = 5\text{Kbits}$, $T_{th} = 3\text{ms}$, and $\mu = 1$.

- [6] K.-K. Wong, A. Shojaefard, K.-F. Tong, and Y. Zhang, "Fluid antenna systems," *IEEE Trans. Wirel. Commun.*, vol. 20, no. 3, pp. 1950–1962, 2020.
- [7] K.-K. Wong, W. K. New, X. Hao, K.-F. Tong, and C.-B. Chae, "Fluid Antenna System—Part I: Preliminaries," *IEEE Commun. Lett.*, 2023.
- [8] A. Dey, R. Guldiken, and G. Mumcu, "Microfluidically reconfigured wideband frequency-tunable liquid-metal monopole antenna," *IEEE Trans. Antennas Propag.*, vol. 64, no. 6, pp. 2572–2576, 2016.
- [9] A. Singh, I. Goode, and C. E. Saavedra, "A multistate frequency reconfigurable monopole antenna using fluidic channels," *IEEE Antennas Wirel. Propag. Lett.*, vol. 18, no. 5, pp. 856–860, 2019.
- [10] S. Song and R. D. Murch, "An efficient approach for optimizing frequency reconfigurable pixel antennas using genetic algorithms," *IEEE Trans. Antennas Propag.*, vol. 62, no. 2, pp. 609–620, 2013.
- [11] L. Tlebaldiyeva, G. Naurzybayev, S. Arzykulov, A. Eltawil, and T. Tsiftsis, "Enhancing QoS through fluid antenna systems over correlated Nakagami- m fading channels," in *2022 IEEE Wireless Commun. Netw. Conf. (WCNC)*. IEEE, 2022, pp. 78–83.
- [12] K. K. Wong, A. Shojaefard, K.-F. Tong, and Y. Zhang, "Performance limits of fluid antenna systems," *IEEE Commun. Lett.*, vol. 24, no. 11, pp. 2469–2472, 2020.
- [13] C. Skouroumounis and I. Krikidis, "Large-scale fluid antenna systems with linear MMSE channel estimation," in *ICC 2022-IEEE Int. Conf. Commun.*. IEEE, 2022, pp. 1330–1335.
- [14] K.-K. Wong and K.-F. Tong, "Fluid antenna multiple access," *IEEE Trans. Wirel. Commun.*, vol. 21, no. 7, pp. 4801–4815, 2021.
- [15] K.-K. Wong, K.-F. Tong, Y. Chen, and Y. Zhang, "Fast Fluid Antenna Multiple Access Enabling Massive Connectivity," *IEEE Commun. Lett.*, 2022.
- [16] K.-K. Wong, D. Morales-Jimenez, K.-F. Tong, and C.-B. Chae, "Slow fluid antenna multiple access," *IEEE Trans. Commun.*, 2023.
- [17] K.-K. Wong, K.-F. Tong, and C.-B. Chae, "Fluid Antenna System—Part III: A New Paradigm of Distributed Artificial Scattering Surfaces for Massive Connectivity," *IEEE Commun. Lett.*, pp. 1–1, 2023.
- [18] Z. Chai, K.-K. Wong, K.-F. Tong, Y. Chen, and Y. Zhang, "Port selection for fluid antenna systems," *IEEE Commun. Lett.*, vol. 26, no. 5, pp. 1180–1184, 2022.
- [19] K. Wong, K. Tong, Y. Chen, and Y. Zhang, "Closed-form expressions for spatial correlation parameters for performance analysis of fluid antenna systems," *Electron. Lett.*, vol. 58, no. 11, pp. 454–457, 2022.
- [20] M. Khammassi, A. Kammoun, and M.-S. Alouini, "A new analytical approximation of the fluid antenna system channel," *IEEE Trans. Wirel. Commun.*, 2023.
- [21] F. R. Ghadi and G. A. Hodtani, "Copula function-based analysis of outage probability and coverage region for wireless multiple access communications with correlated fading channels," *IET Commun.*, vol. 14, no. 11, pp. 1804–1810, 2020.
- [22] E. A. Jorswieck and K.-L. Besser, "Copula-based bounds for multi-user communications—Part I: Average Performance," *IEEE Commun. Lett.*, vol. 25, no. 1, pp. 3–7, 2020.
- [23] F. R. Ghadi and G. A. Hodtani, "Copula-based analysis of physical layer security performances over correlated Rayleigh fading channels," *IEEE Trans. Inf. Forensics Secur.*, vol. 16, pp. 431–440, 2020.
- [24] K.-L. Besser, P.-H. Lin, and E. A. Jorswieck, "On fading channel dependency structures with a positive zero-outage capacity," *IEEE Trans. Commun.*, vol. 69, no. 10, pp. 6561–6574, 2021.
- [25] F. R. Ghadi, F. J. Martin-Vega, and F. J. López-Martínez, "Capacity of backscatter communication under arbitrary fading dependence," *IEEE Trans. Veh. Technol.*, vol. 71, no. 5, pp. 5593–5598, 2022.
- [26] K.-L. Besser and E. A. Jorswieck, "Bounds on the secrecy outage probability for dependent fading channels," *IEEE Trans. Commun.*, vol. 69, no. 1, pp. 443–456, 2020.
- [27] F. R. Ghadi and W.-P. Zhu, "Performance Analysis Over Correlated/Independent Fisher-Snedecor \mathcal{F} Fading Multiple Access Channels," *IEEE Trans. Veh. Technol.*, vol. 71, no. 7, pp. 7561–7571, 2022.
- [28] I. Trigui, D. Shahbazzabar, W. Ajib, and W.-P. Zhu, "Copula-Based Modeling of RIS-Assisted Communications: Outage Probability Analysis," *IEEE Commun. Lett.*, vol. 26, no. 7, pp. 1524–1528, 2022.
- [29] F. R. Ghadi, F. J. López-Martínez, W.-P. Zhu, and J.-M. Gorce, "The Impact of Side Information on Physical Layer Security Under Correlated Fading Channels," *IEEE Trans. Inf. Forensics Secur.*, vol. 17, pp. 3626–3636, 2022.
- [30] K.-L. Besser and E. A. Jorswieck, "Reliability bounds for dependent fading wireless channels," *IEEE Trans. Wirel. Commun.*, vol. 19, no. 9, pp. 5833–5845, 2020.
- [31] F. R. Ghadi and F. J. López-Martínez, "RIS-Aided Communications over Dirty MAC: Capacity Region and Outage Probability," *IEEE Communications Letters*, 2023.
- [32] F. R. Ghadi, K.-K. Wong, F. J. Lopez-Martinez, and K.-F. Tong, "Copula-based Performance Analysis for Fluid Antenna Systems under Arbitrary Fading Channels," *arXiv preprint arXiv:2305.09553*, 2023.
- [33] G. Frahm, M. Junker, and A. Szimayer, "Elliptical copulas: applicability and limitations," *Stat. Probab. Lett.*, vol. 63, no. 3, pp. 275–286, 2003.
- [34] G. L. Stüber and G. L. Stüber, *Principles of mobile communication*. Springer, 2001, vol. 2.
- [35] R. B. Nelsen, *An introduction to copulas*. Springer science & business media, 2007.
- [36] H.-C. Yang, S. Choi, and M.-S. Alouini, "Ultra-reliable low-latency transmission of small data over fading channels: A data-oriented analysis," *IEEE Commun. Lett.*, vol. 24, no. 3, pp. 515–519, 2019.
- [37] A. Genz and F. Bretz, "Numerical computation of multivariate t-probabilities with application to power calculation of multiple contrasts," *J. Stat. Comput. Simul.*, vol. 63, no. 4, pp. 103–117, 1999.
- [38] —, "Comparison of methods for the computation of multivariate t

- probabilities,” *J. Comput. Graph. Stat.*, vol. 11, no. 4, pp. 950–971, 2002.
- [39] X. Wei, D. Han, and X. Du, “Approximation to multivariate normal integral and its application in time-dependent reliability analysis,” *Struct. Saf.*, vol. 88, p. 102008, 2021.
- [40] J.-F. Mai and M. Scherer, *Simulating copulas: stochastic models, sampling algorithms, and applications*. Imperial College Press, 2017, vol. 6.